Diffusion properties of asymptomatic lumbar intervertebral discs in a pediatric cohort: a preliminary study of apparent diffusion coefficient

Roxane Compagnon, Baptiste Brun-Cottan, Pauline Assemat, Julie Vial, Jérôme Sales de Gauzy, Pascal Swider

Diffusion properties of asymptomatic lumbar intervertebral discs in a pediatric cohort; a preliminary study of apparent diffusion coefficient

[1.2, *]Roxane Compagnon MD MSc
[2] Baptiste Brun-Cottan PhD
[2] Pauline Assemat PhD
[1]Julie Vial MD
[1.2] Professor Jérôme Sales de Gauzy MD
[2]Professor Pascal Swider PhD

From:
1 - Children Hospital, Toulouse, France
2 - IMFT UMR CNRS 5502. Toulouse University, CHU Purpan, Toulouse, France

* Now at Clinique Médipôle Garonne, Toulouse, France

Corresponding author:
Professor Pascal Swider, PhD
IMFT UMR CNRS 5502. Toulouse University, CHU Purpan, Toulouse, France
2 allées C. Soula
31400
France
Email : pascal.swider@imft.fr

Abstract

Purpose: To explore the apparent diffusion coefficients of intervertebral discs in an asymptomatic pediatric cohort.
Methods: We conducted a prospective MRI study of the lumbar spine from below the thoracolumbar junction to the lumbosacral junction on 12 subjects (mean age 13 y.o.) with no spinal pathology or spinal posture disorder. MRI imaging was carried out using a 1.5 T machine with acquisitions realized both in sagittal and coronal planes. First, disc hydration was determined and then, diffusion-weighted images (DWI) were obtained using an SE single-shot echo-planar sequence. Apparent diffusion coefficients (ADC) of anterior annulus fibrosus (AAF), nucleus pulposus (NP) and posterior annulus fibrosus (PAF) were measured in the sagittal plane.
Results: Averaged hydration of 0.27 SD 0.03 confirmed the asymptomatic nature of discs. Average scaled values of ADC were 0.46 SD 0.01, 0.22 SD 0.09 and 0.18 SD 0.03 for NP, AAF and PAF, respectively. ADC of NP were almost constant along the spine, PAF values show a slight increase in the thorax-sacrum direction while AAF values showed a pronounced decrease. Locally, ADC of AAF was higher compared to ADC PAF values below the thoracolumbar junction and it reversed for subjacent discs.
Conclusions: In our knowledge, our study provided the first diffusive properties of asymptomatic intervertebral discs in an adolescent cohort. ADC of NP was slightly higher than adults'. ADC evolutions of AAF were correlated with lordosis concavity which pointed out the role of

compressive strain on fluid transport properties. This study could furnish information about segment homeostasis for exploration of pediatric spinal pathologies.

Disclosure of interest
The authors declare that they have no competing interest.

Funding
Fondation Cotrel (Institut de France)

Author contributions
Roxane Compagnon: study design, study design, data analysis, and writing of article and validation of submitted version.
Baptiste Brun- Cottan: data analysis and validation of submitted version of article.
Julie Vial: data acquisition, Roxane Compagnon contributed data analysis or interpretation (…).
Pauline Assemat: data analysis and interpretation, validation of submitted version.
Jérôme Sales de Gauzy: study design, validation of submitted version
Pascal Swider: study design, data analysis and interpretation, writing of article and validation of submitted version.

Acknowledgements
We are grateful to the Fondation Cotrel (Institut de France) for its on-going support of our research on idiopathic scoliosis. We thank SFCR (Société Française de chirurgie Rachidienne) for R. Compagnon's scholarship (MD). We are grateful to C. Baunin MD who managed MRI data collection. We are grateful to Jérôme Briot PhD, who developed the Biomechlab® software.

1 - Introduction

The inter-vertebral disc (IVD) is a large avascular fibrocartilaginous structure organized in three anatomical zones: the nucleus pulposus (NP) or internal complex, the annulus fibrosus (AF) and the cartilage end plates (CEP) [1]. The microarchitecture of the interface between NP and AF is diffuse but components of extracellular matrix can be distinguished. NP is constituted of a network of type-2 collagen involving proteoglycans which negative charged molecules ensure a significant hydration level. The cell fraction limited to 4000 cells/mm3, mainly concerns chondrocytes and fibrocytes. AF is constituted of tight and well-organized fibers of type-1 collagen with a weak proportion of proteoglycans and very low cellularity. CEP is constituted of a thick layer of hyaline cartilage permeable to small molecules, fluid and ions with an average cell fraction of 15000 cells/mm3. Water fraction represents 65 % to 90 % of the IVD volume and varies with diurnal cycle [1], [2].

In fetal life and childhood until 2 years, IVD nutrition is supported by blood vessels from vertebrae through CEP. Then, this vascular supply decreases to almost disappear at puberty and the main nutritional support is maintained by convection and diffusion of fluid and micro nutriments. Nutritional alterations associated to biophysical IVD changes in adults are deeply investigated. This tends to conclude that disc degeneration is a continuum, starting from the second decade of life [3], [4].

Magnetic Resonance Imaging (MRI) is an imaging modality used to explore soft tissues hydration [5], [6] and specifically disc degeneration signs [3]. Main sequences based on signal relaxation time, i.e. T1 or T2, which discriminate specific tissue responses are associated to STIR imaging (Short Tau Inversion Recovery), in which fat components are filtered. Diffusion weighted imaging (DWI) allows describing the diffusion of free water molecules [7]. Based on an echo-planar spin echo sequence (EPI-SE), DWI adds specific magnetic gradients before and after the 180° radio frequency impulsion and it results in hyper-signal in low molecular diffusion zones and hypo-signal in high molecular diffusion zones. The apparent diffusion coefficient (ADC) is a scalar measure of the magnitude of molecular diffusion obtained from DWI. In living tissue, diffusion is restricted by cells and extra cellular matrix components and lower to that of free water equal to 3×10^{-3} mm^2/s.

Concerning IVD, the literature review in adults showed large discrepancies of ADC mainly due to non-standardized protocols. DWI sequences and region of interest (ROI) are varying significantly. Indeed, often focused on NP center, the ROI surface can fluctuate between 2 mm^2 and 110 mm^2 [8]-[10]. Signals may intersect several tissues, a complexity which induces bias in the outcome standardization and frequently, a unique value is proposed whereas IVD is a complex multi-tissue structure. Despite these limitations, ADC range can be considered between 1.22 and 2.46×10^{-3} mm^2/s for asymptomatic IVD in adults with lower values for caudal discs [8]-[11]. Discs with degeneration signs show increased values of ADC correlated with age, disc level, Pfirrmann grade but not gender [3],[8],[9],[11]-[16]. This could reveal the potential presence of freely moving fluid contained within structural change, such as cracks and cavities. Some ADC of NP in adults and young adults, summarized in Table 1, show that values for asymptomatic discs are comprised between 1.2 and 2.35×10^{-3} mm^2/s and values for degenerative discs are comprised between 1.4 and $2.22.10^{-3}$ mm^2/s.

Much more is known in IVD aging than of the evolving properties during maturation [17],[20]. Furthermore, disabling pediatric diseases such as idiopathic scoliosis or spondylolisthesis might impact segment homeostasis and their roles in surgical outcomes. Indeed, the sagittal organization may have a leading role in pre- and post-operative behavior of lumbar discs [21]-[23]. In this

context, completing control data can be clinically relevant and for this purpose, we measured diffusion properties of intervertebral discs in an asymptomatic children cohort. We hypothesized that variation of ADC differentiated according to disc structural components and localization had to be considered.

2 - Methods

The study included 12 consecutive subjects who underwent a spinal MRI. The collection of imaging exams was performed in accordance with the protocol approved by the Ethics Committee of University Children Hospital of Toulouse (France). Inclusion criteria were: a) age comprises between 7 and 20 years inclusive, b) no spinal pathology or spinal posture disorder diagnosed on MRI after validation by a pediatric imaging specialist. The mean age of the included subjects was 13.3 years (SD = 2.92) and our evaluation focused on the lumbar spine from below the thoracolumbar junction, i.e. L_1-L_2, to the lumbosacral junction, i.e. L_5-S_1.

MRI Imaging was carried out using a 1.5-T Toshiba Vantage Titan machine with both sagittal and coronal scans. The sagittal scans were as follows: gradient echo TR/TE 5.2/2.6 ms, slice thickness 10.0 mm, spacing 8.0 mm, field of view 30×25 cm, and matrix size 192×192. The coronal scans were as follows: gradient echo (GE), TR/TE: 5.2/2.6 ms, slice thickness 10.0 mm, spacing : 8.0 mm, field of view (FOV) 37×30 cm, and matrix size 192 ×192.

On T2 and STIR imaging, the IVD and NP volumes were reconstructed using dedicated image processing software developed with Matlab®. Disc segmentation was achieved using a tactile device Wacom® Cintiq 21 UX. Disc hydration was defined as the ratio between NP volume and disc volume [22]. Lumbar discs L_1-L_2 to L_5-S_1 were studied, as shown in Figure 1a.

The diffusion-weighted images (DWI) were obtained using an SE single-shot echo-planar (EPI-SE) sequence as follows: TR/TE: 2727/100 ms, slice thickness: 5 mm, spacing: 5 mm, field of view: 37 ×30 cm, matrix size: 128×128, and number of excitation: 1. The diffusion-sensitizing gradients were applied sequentially in the *x*-, *y*-, and *z*-directions, *z* corresponding to main magnetic field and patient longitudinal axis.

The signal decrease is described by exponential expression (1a) where S_0 is the baseline signal intensity and S_b is the signal intensity with applied diffusion gradients. The ADC is deducted from (1a) and expressed by equation (1b) with the diffusion-weighting factor associated with S_b so-called *b*-value. This value fixed to b = 600 s/mm^2 provided a good compromise between resolution and acquisition time of 132s, for the studied cohort.

$$S_b = S_0 \cdot e^{-b \cdot ADC} \text{ (a)} \Leftrightarrow ADC = -\frac{1}{b} \cdot \ln \frac{S_b}{S_0} \text{ (b)} \quad (1)$$

Offline image analysis software was used to analyze maps of ADC (OsiriX DICOM software V2.31) in the sagittal plane. Three regions of interest (ROI) per disc were defined and located in anterior annulus fibrosus (AAF), nucleus pulposus (NP) and posterior annulus fibrosus (PAF). The circular ROI size was 10 mm^2 corresponded to a diameter of 3.57 mm.

In the antero-posterior direction, AAF and PAF matched with lowest intensity signals of DW-EPI image, whereas NP matched with highest intensity. Along the local cranio-caudal axis, the three ROI were located at mid-distance of the top and bottom CEP. Initially, the S_0 value maps were registered and then S_{600} value maps were superimposed while saving locations of ROI. Finally, equation (1b) was used to compute ADC values using integrated values of S_0 and S_{600} into each ROI.

3 - Results

The determination of ADC value was achieved three times for each ROI segmentation in each sagittal maps and the reproducibility error was lower than 2 %.

The structure of discs was homogeneous with bright hyper intense white signal intensity and a normal disc height, as shown in Figure 1a. The cohort was ranked grade I (A) in Pfirrmann classification [3].

Volumes of lumbar discs and NP were determined after segmentation of frontal and sagittal T2 images as shown in Figure 1b, and the averaged hydration of 0.27 SD 0.03 was obtained for L_1-L_2 to L_5-S_1 discs. The STIR image shown in Figure 1c associated with the DW-EPI intensity map of Figure 1d are provided as imaging data type. The resulting ADC of the cohort and and mean values per vertebral level are presented in Tables 2a, 2b and 2c. Mean ADC for AAF, NP and PAF for the whole spine were 2.22 mm^2/s SD 0.04, 1.04 mm^2/s SD 0.41 and 0.87 mm^2/s SD 0.15, respectively.

Using ADC value of cerebrospinal fluid as reference, i.e. 4.18×10^{-3} mm^2/s measured at L_3 location, statistical distribution of scaled ADC for NP, AAF and PAF are plotted in Figure 2 from L_1-L_2 to L_5-S_1. Mean values were 0.46 SD 0.01, 0.22 SD 0.09 and 0.18 SD 0.03, respectively. Standard deviations were minimal for NP and maximal for AAF. The difference between average ADC values of NP and AF per vertebral segment was significant with a t-test p-value of 7.1×10^{-5}.

Evolutions of scaled ADC magnitude along the lumbar spine are shown in Figure 3 using longitudinal distance between L_1-L_2 and L_5-S_1 to describe the scaled path. Cubic polynomial interpolation were associated and coefficients were (0.11, -0.16, 0.07, 0.45) for NP, (1.1, -1.8, 0.55, 0.27) for AAF and (-0.05, 0.14, -0.01, 0.15). It showed that ADC values of NP were almost constant, PAF values show a slight increase and AAF values showed more variations and a global pronounced decrease. Minimal value of the coefficient of determination r^2 was 0.96.

Figure 4 shows the distribution of average scaled ADC along the local antero-posterior axis of discs. ADC value of NP and AAF - PAF distance are used to scale ADC magnitudes and path, respectively and a quadratic polynomial curve fitting was associated. AAF values show largest variations whereas PAF values are more constant. Indeed, ratios vary from one quarter to two third for AAF and about one third for PAF. Compared to PAF values, AAF values are higher for L_1-L_2 and L_2-L_3 but they reverse from L_3-L_4 to L_5-S_1. This is accompanied by the shift of distribution patterns associated with the NP migration toward the posterior direction.

4 - Discussion and conclusion

The aim was to explore diffusion properties of asymptomatic discs in a children cohort. According to our initial assumption, we found significant evolution of ADC internal to the discs and along the lumbar longitudinal axis.

Disc volume reconstruction and hydration calculations from T2 sequences confirmed the asymptomatic nature of discs [3] since included in the range of normality [15]. ADC of nucleus pulposus was almost constant and slightly higher than adults' while being in the range of overall intervertebral disc values proposed in the literature as summarized in Table 1. Evolution of ADC can be associated to variation of free water content likewise water in an extracellular compartment. Free water content also can reflect the quality of nutrient supply, as a consequence of efficient exchanges between disc and vertebra, and this was confirmed by the higher values compared to adults found at the nucleus pulposus location.

The overlapping ADC values in Table 1 may be due to the natural variation of tissue properties whether they are asymptomatic or degenerated but also to non-standardized protocols assuming

that all MR scanners were calibrated. Indeed, b -values, ROI shapes, sizes and location showed significant variations. Our protocol did not aim at defining a pediatric norm but at furnishing values of a pediatric cohort explored using a methodology usable in clinical setting.

In this framework, we found that ADC of annulus fibrosus was significantly lower than that of the nucleus pulposus. In addition, variations were associated with the evolution of lumbar lordosis towards the spino-pelvic alignment. Indeed, reversed ADC evolutions of anterior and posterior annulus fibrosus were correlated with the relative inclination of vertebral plateaus. It was found that ADC was weaker in the lordosis concavity, especially in AAF, and this pointed out that compressive strain could influence locally transport properties into the disc. Here, we could suggest that common exploration of differentiated diffusive properties and location-dependent biomechanical loadings and energies [24] could be considered to explore the segment homeostasis and beyond, to study the bifurcation towards pathological behavior.

The methodology involving imaging protocol and associated post-treatment was designed to ensure a compromise between accuracy and feasibility in pediatric clinical setting. The annulus fibrosus being a fibrous structure, diffusion tensor imaging could potentially inform about the location-dependent anisotropic properties. Unfortunately, additional series of sequences and increased examination time were prohibitive with our pediatric cohort.

Main limitation of our study concerned the limited number of subjects (and centers) and therefore it should be considered as a preliminary study. We suggested that evolution of ADC of discs could be described a polynomial form in the global reference of the spine. The interpolation degree sufficiently high, allowed physiological oscillations according to the spine anatomy to be predicted. In our knowledge, our study provided the first diffusive properties of asymptomatic intervertebral discs in an adolescent population with additional information about their spatial heterogeneity. T2 imaging reflects total water content and ADC evolution can be associated to variation of free water content. Their coupling could furnish information about segment homeostasis for early diagnosis, surgical outcome and patient follow-up in pathologies such as idiopathic scoliosis or spondylolisthesis.

References

[1] Urban, J. P. and C. P. Winlove (2007). Pathophysiology of the intervertebral disc and the challenges for MRI. *Journal of Magnetic Resonance Imaging 25* (2), 419–432.

[2] Ludescher, B., J. Effelsberg, P. Martirosian, G. Steidle, B. Markert, C. Claussen, and F. Schick (2008). T2- and diffusion-maps reveal diurnal changes of intervertebral disc composition: An in vivo MRI study at 1.5 Tesla. *Journal of Magnetic Resonance Imaging 28* (1), 252–257.

[3] Pfirrmann, C. W., A. Metzdorf, M. Zanetti, J. Hodler, and N. Boos (2001). Magnetic resonance classification of lumbar intervertebral disc degeneration. *Spine 26* (17), 1873–1878.

[4] Yu, H. J., S. Bahri, V. Gardner, and L. T. Muftuler (2014). In vivo quantification of lumbar disc degeneration: assessment of ADC value using a degenerative scoring system based on Pfirrmann framework. European Spine Journal, 1–7.

[5] Brown, M. A. and R. C. Semelka (2010). *MRI: basic principles and applications* (4th ed ed.). Hoboken, N.J: Wiley-Blackwell/John Wiley & Sons.

[6] Botchu R, Bharath A, Davies AM, Butt S, James SL (2018). Current concept in upright spinal MRI. Eur Spine J. 27(5):987-993.

[7] Le Bihan D. Apparent diffusion coefficient and beyond: what diffusion MR imaging can tell us about tissue structure (2013). Radiology 268(2):318–22. 10.1148/radiol.13130420

[8] Wu, N., H. Liu, J. Chen, L. Zhao, W. Zuo, Y. Ming, S. Liu, J. Liu, X. Su, B. Gao, Z. Tang, G. Qiu, G. Ma, and Z. Wu (2013). Comparison of Apparent Diffusion Coefficient and T2 Relaxation Time Variation Patterns in Assessment of Age and Disc Level Related Intervertebral Disc Changes. *PLoS ONE 8* (7).
[9] Zhang, W., X. Ma, Y. Wang, J. Zhao, X. Zhang, Y. Gao, and S. Li (2014). Assessment of apparent diffusion coefficient in lumbar intervertebral disc degeneration. *European Spine Journal. 23* (9), 1830–1836.
[10] Shen, S., H. Wang, J. Zhang, F. Wang, and S.-R. Liu (2016). Diffusion Weighted Imaging, Diffusion Tensor Imaging, and T2* Mapping of Lumbar Intervertebral Disc in Young Healthy Adults. Ir. Journal of Radiology 13.
[11] Kealey, S. M., T. Aho, D. Delong, D. P. Barboriak, J. M. Provenzale, and J. D. Eastwood (2005). Assessment of apparent diffusion coefficient in normal and degenerated intervertebral lumbar disks: initial experience. 2000. *Radiology 235* (2), 569–574.
[12] Niu, G., X. Yu, J. Yang, R. Wang, S. Zhang, and Y. Guo (2011). Apparent diffusion coefficient in normal and abnormal pattern of intervertebral lumbar discs: initial experience. *Journal of Biomedical Research 25* (3), 197–203.
[13] Antoniou, J., C. N. Demers, G. Beaudoin, T. Goswami, F. Mwale, M. Aebi, and M. Alini (2004). Apparent diffusion coefficient of intervertebral discs related to matrix composition and integrity. *Magnetic Resonance Imaging 22* (7), 963–972.
[14] Tokuda, O., M. Okada, T. Fujita, and N. Matsunaga (2007). Correlation between diffusion in lumbar intervertebral disks and lumbar artery status: evaluation with fresh blood imaging technique. *Journal of magnetic resonance imaging: JMRI 25* (1), 185–191.
[15] Jarman JP, Arpinar VE, Baruah D, Klein AP, Maiman DJ, Muftuler LT (2015). Intervertebral disc height loss demonstrates the threshold of major pathological changes during degeneration. Eur Spine J. 24(9):1944-50.
[16] Yu HJ, Bahri S, Gardner V, Muftuler LT (2015). In vivo quantification of lumbar disc degeneration: assessment of ADC value using a degenerative scoring system based on Pfirrmann framework. Eur Spine J. 24(11):2442-8.
[17] Kerttula LI, Jauhiainen JP, Tervonen O, Suramo IJ, Koivula A, Oikarinen JT (2000). Apparent diffusion coefficient in thoracolumbar intervertebral discs of healthy young volunteers. J Magn Reson Imaging. 12(2):255-60.
[18] Wong AYL, Parent EC, Dhillon SS, Prasad N, Samartzis D, Kawchuk GN (2019). Differential patient responses to spinal manipulative therapy and their relation to spinal degeneration and post-treatment changes in disc diffusion. Eur Spine J. 28(2):259-269.
[19] Krueger EC, Perry JO, Wu Y, Haughton VM. Changes in T2 relaxation times associated with maturation of the human intervertebral disk (2007). AJNR Am J Neuroradiol 28(7):1237-41.
[20] Bolzinger M, Estivalèzes E, Gallini A, Polirsztok E, Abelin-Genevois K, Baunin C, Sales de Gauzy J, Swider P.(2020). MRI evaluation of the hydration status of non-pathological lumbar intervertebral discs in a pediatric population. Orthop Traumatol Surg Res. 106(7):1281-1285.
[21] Green DW, Lawhorne TW 3rd, Widmann RF, Kepler CK, Ahern C, Mintz DN, Rawlins BA, Burke SW, Boachie-Adjei O. Long-term magnetic resonance imaging follow-up demonstrates minimal transitional level lumbar disc degeneration after posterior spine fusion for adolescent idiopathic scoliosis (2011). Spine (Phila Pa 1976) 36(23):1948-54.
[22] Gervais J, Périé D, Parent S, Labelle H, Aubin CE (2012). MRI signal distribution within the intervertebral disc as a biomarker of adolescent idiopathic scoliosis and spondylolisthesis. BMC Musculoskelet Disord. 3;13:239.

[23] Abelin-Genevois K, Estivalezes E, Briot J, Sévely A, Sales de Gauzy J, Swider P. 2015. Spino-pelvic alignment influences disc hydration properties after AIS surgery: a prospective MRI-based study. Eur Spine J.;24(6):1183-90.
[24] Brun-Cottan B, Assemat P, Doyeux V, Accadbled F, Sales de Gauzy J, Compagnon R, Swider P. 2021. An energy approach describes spine equilibrium in adolescent idiopathic scoliosis. Biomech Model Mechanobiol. 20(1):359-370.

Captions for tables and illustrations

Table 1: ADC in nucleus pulposus (10^{-3} mm^2/s) of adult and young adult population

Table 2: ADC ($\times 10^{-3}$ mm^2/s) in our pediatric cohort ($n = 12$): a - nucleus pulposus (NP), **b -** anterior annulus fibrosus (AAF), **c -** posterior annulus fibrosus (PAF)

Figure 1 – Lumbar MR imaging in the sagittal plane: **(a)** T2 imaging, **(b)** Semi-automated segmentation and automated volume reconstruction of IVD from MRI slices using tactile device Wacom® Cintiq 21 UX, (c) STIR imaging, (d) Map of ADC (10^{-6} mm^2/s, grayrainbow clut) showing ROIs in nucleus pulposus (NP), anterior annulus fibrosus (AAF) and posterior annulus fibrosus (PAF).

Figure 2- Box-plots of average dimensionless ADC: **(a)** ADC of anterior annulus fibrosus (AAF), **(b)** ADC of nucleus pulposus (NP), **(c)** ADC of posterior annulus fibrosus (PAF). Values are scaled using the ADC of cerebrospinal fluid at L_3 (4.18×10^{-3} mm^2/s).

Figure 3 - Evolution of average dimensionless ADC of nucleus pulposus (NP), anterior annulus fibrosus (AAF) and posterior annulus fibrosus (PAF) from below the thoracolumbar junction, i.e. L_1-L_2 to lumbosacral junction, i.e. L_5-S_1. ADC values are scaled using the ADC of cerebrospinal fluid (4.18×10^{-3} mm^2/s) at L_3. Disc co-ordinates are scaled using L_1-L_2, L_5-S_1 distance.and cubic polynomial curve fittings are associated.

Figure 4 - Evolution of average dimensionless ADC of nucleus pulposus (NP), anterior annulus fibrosus (AAF) and posterior annulus fibrosus (PAF) along local antero-posterior path of L_1-L_2 to L_5-S_1 discs. ADC values are scaled using ADC of local nucleus pulposus. Local co-ordinates are scaled using AAF, PAF distance and quadratic polynomial curve fittings are associated.

reference	ex-vivo	asymptomatic	degeneration	ADC
Kerttula et al. (2000)		x		1.2 - 1.8
Antoniou et al. (2004)	x			1.1 - 1.3
Kealey et al. (2005)		x		1.97 - 2.35
			x	1.72 - 2.22
Tokuda et al. (2007)		x		1.94
Ludescher et al. (2008)		x		1.2 - 2.2
Wu et al. (2013)		x		1.9
Jarman et al. (2014)		x		1.5
Yu et al. (2014)		x		1.61 - 1.81
Zhang et al. (2014)			x	1.4 - 1.6
Shen et al. (2016)		x		1.93 - 2.17
Wong et al. (2019)			x	2.08 - 2.26

Table 1: ADC values of nucleus pulposus (10^{-3} mm^2/s) of adult and young adult population

a - NP	Subjects												
	#1	#2	#3	#4	#5	#6	#7	#8	#9	#10	#11	#12	mean
L1/L2	2.10	2.88	1.70	2.19	2.23	2.65	2.49	2.37	2.10	2.20	2.27	2.13	2.28 SD 0.3
L2/L3	2.22	2.82	2.15	2.25	2.42	2.40	2.62	2.48	2.16	2.29	2.34	2.10	2.35 SD 0.21
L3/L4	2.19	2.45	1.97	2.13	2.11	2.24	2.38	2.27	2.08	2.21	2.38	2.13	2.21 SD 0.14
L4/L5	2.10	2.31	1.78	2.26	2.36	2.22	2.28	2.26	2.21	2.33	2.45	2.01	2.21 SD 0.18
L5/S1	2.08	2.10	1.97	2.26	2.19	2.55	1.83	2.19	2.08	2.29	2.51	1.98	2.17 SD 0.21
b - AAF													
L1/L2	0.38	0.06	0.50	0.38	0.22	1.05	0.97	0.32	0.93	0.56	0.71	0.81	0.57 SD 0.32
L2/L3	0.83	0.10	0.60	0.45	0.99	0.81	0.89	0.25	0.84	0.41	0.88	0.43	0.66 SD 0.26
L3/L4	0.74	1.50	1.10	1.80	0.52	1.46	1.53	1.09	0.86	0.20	1.71	0.83	1.11 SD 0.50
L4/L5	1.03	1.90	1.50	1.76	1.42	1.86	1.81	0.92	2.56	1.35	1.90	1.15	1.53 SD 0.36
L5/S1	1.38	1.31	1.20	1.29	1.32	1.22	1.34	0.97	1.44	1.81	1.86	0.49	1.30 SD 0.35
c- PAF													
L1/L2	0.56	2.05	1.10	0.97	1.04	1.30	1.10	0.94	1.07	0.58	0.98	1.30	1.08 SD 0.38
L2/L3	1.22	0.69	0.90	0.42	1.04	1.17	0.77	0.78	0.95	1.16	1.23	0.70	0.92 SD 0.26
L3/L4	1.55	0.57	0.85	0.21	0.85	1.47	0.43	0.80	0.55	1.13	1.15	0.91	0.87 SD 0.40
L4/L5	1.19	0.49	0.70	0.27	0.03	1.29	0.55	1.16	0.35	1.30	0.95	0.31	0.72 SD 0.45
L5/S1	0.97	0.59	0.68	0.33	0.70	1.57	0.65	0.54	0.64	0.71	0.81	0.64	0.74 SD 0.30

Table 2: ADC ($\times 10^{-3}$ mm^2/s) in the pediatric cohort (n = 12): a - nucleus pulposus (NP), **b -** anterior annulus fibrosus (AAF), **c -** posterior annulus fibrosus (PAF)

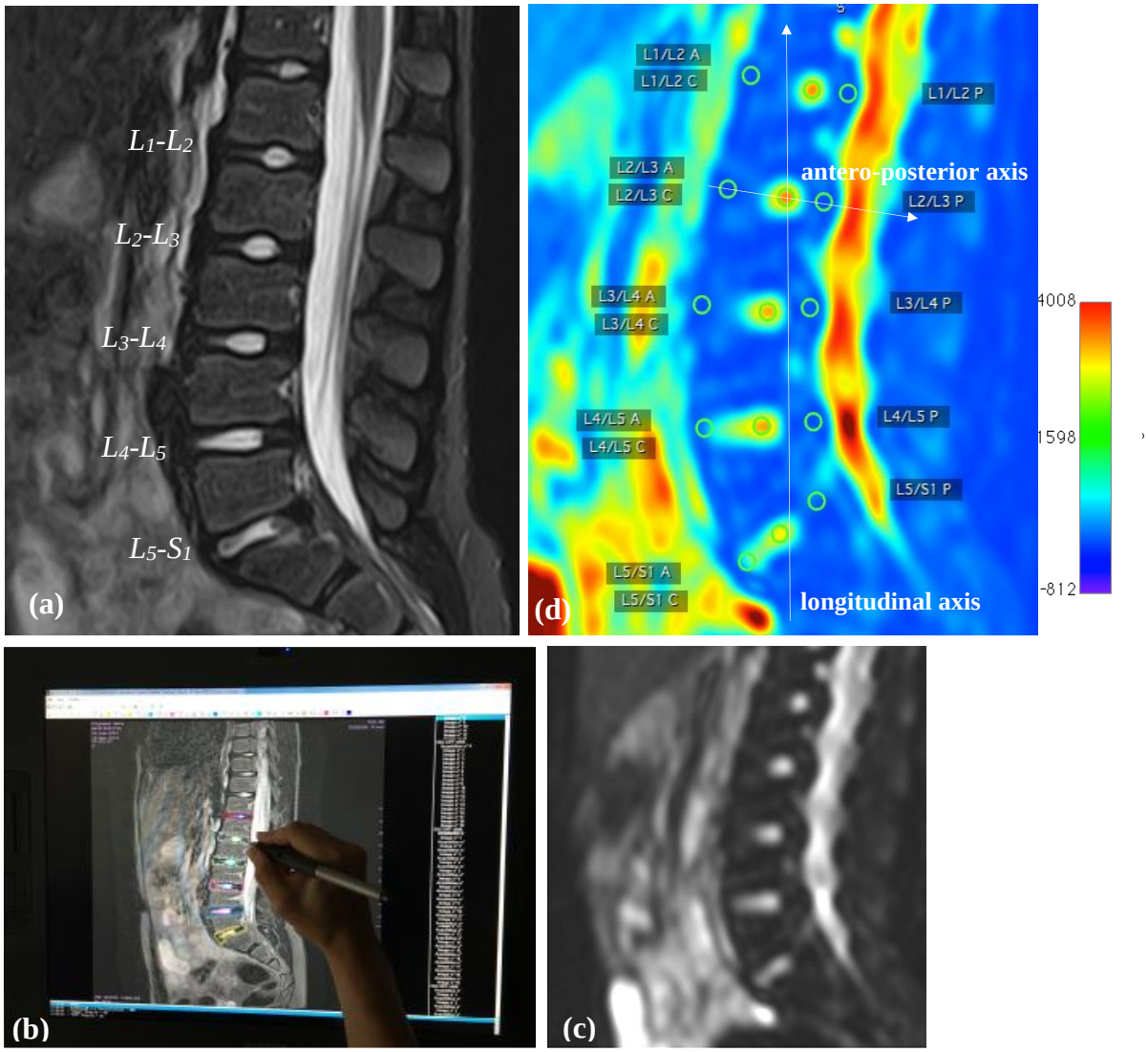

Figure 1 – Lumbar MR imaging in the sagittal plane: **(a)** T2 imaging, **(b)** Semi-automated segmentation and automated volume reconstruction of IVD from MRI slices using tactile device Wacom® Cintiq 21 UX, **(c)** STIR imaging, **(d)** Map of ADC (10^{-6} mm^2/s, *grayrainbow clut*) showing ROIs in nucleus pulposus (NP), anterior annulus fibrosus (AAF) and posterior annulus fibrosus (PAF).

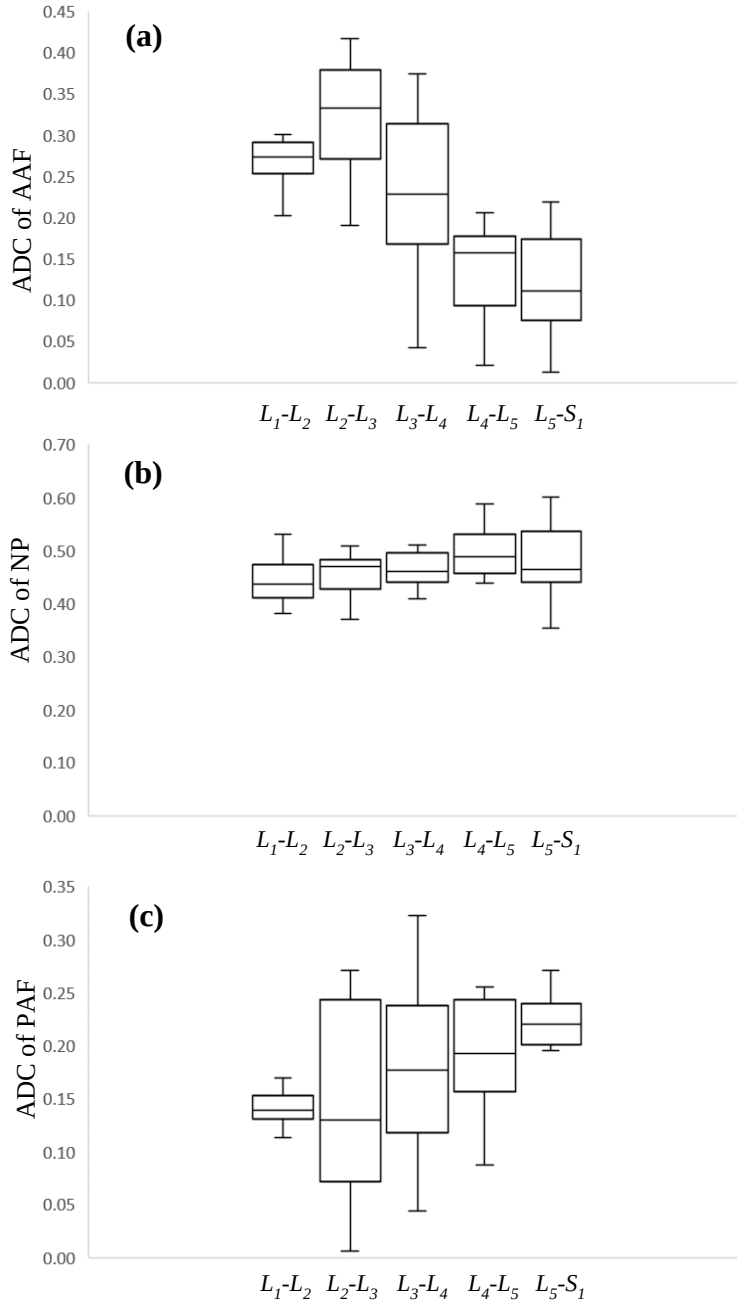

Figure 2- Box-plots of average dimensionless ADC: **(a)** ADC of anterior annulus fibrosus (AAF), **(b)** ADC of nucleus pulposus (NP), **(c)** ADC of posterior annulus fibrosus (PAF). Values are scaled using the ADC of cerebrospinal fluid at L_3 (4.18×10^{-3} mm^2/s).

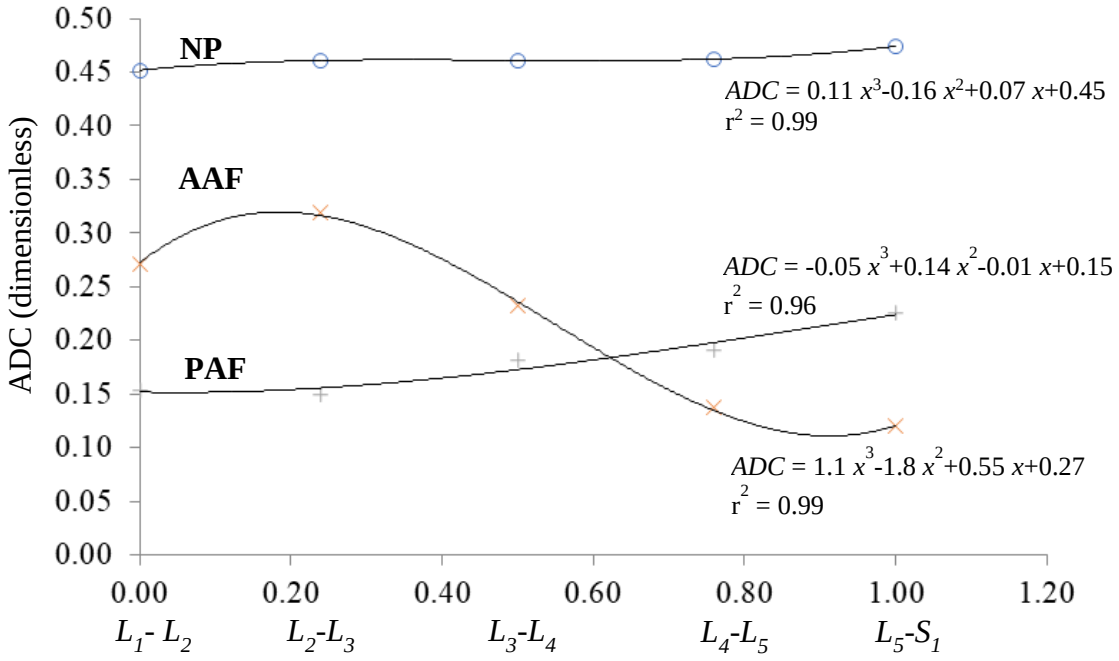

Figure 3 - Evolution of average dimensionless ADC of nucleus pulposus (NP), anterior annulus fibrosus (AAF) and posterior annulus fibrosus (PAF) from below the thoracolumbar junction, i.e. L_1-L_2 to lumbosacral junction, i.e. L_5-S_1. ADC values are scaled using the ADC of cerebrospinal fluid (4.18×10^{-3} mm^2/s) at L_3. Disc co-ordinates are scaled using L_1-L_2, L_5-S_1 distance.and cubic polynomial curve fittings are associated.

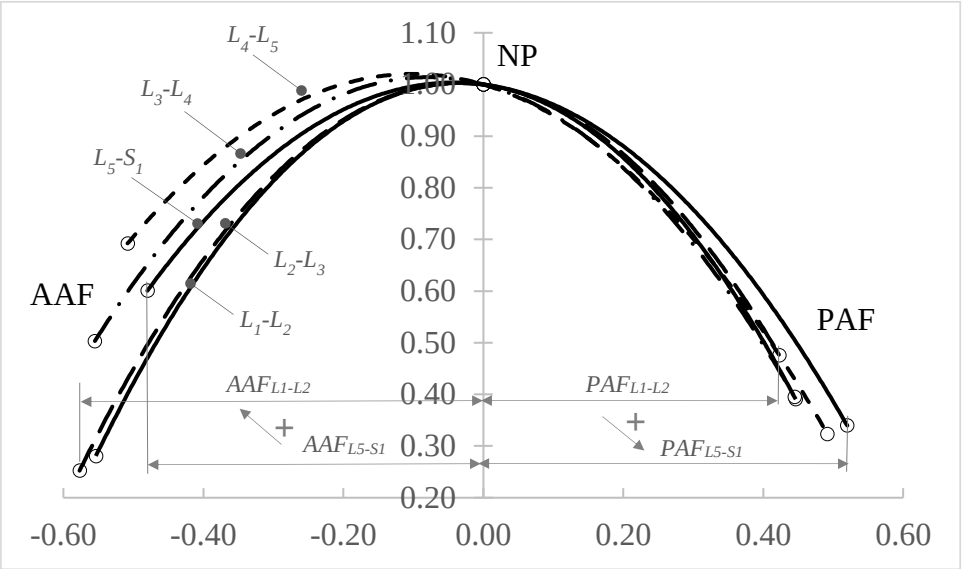

Figure 4 - Evolution of average dimensionless ADC of nucleus pulposus (NP), anterior annulus fibrosus (AAF) and posterior annulus fibrosus (PAF) along local antero-posterior path of L_1-L_2 to L_5-S_1 discs. ADC values are scaled using ADC of local nucleus pulposus. Local co-ordinates are scaled using AAF, PAF distance and quadratic polynomial curve fittings are associated.